

# Mechanistic investigation into the light soaking effect observed in inverted polymer solar cells containing chemical bath deposited titanium oxide

メタデータ	言語: eng 出版者: 公開日: 2017-10-03 キーワード (Ja): キーワード (En): 作成者: メールアドレス: 所属:
URL	<a href="https://doi.org/10.24517/00010776">https://doi.org/10.24517/00010776</a>

This work is licensed under a Creative Commons Attribution-NonCommercial-ShareAlike 3.0 International License.



# Mechanistic Investigation into the Light Soaking Effect Observed in Inverted Polymer Solar Cells Containing Chemical Bath Deposited Titanium Oxide

Takayuki Kuwabara <sup>\*†‡</sup>, Katsuhiko Yano <sup>†</sup>, Takahiro Yamaguchi <sup>†</sup>, Tetsuya Taima <sup>†‡§</sup>,  
Kohshin Takahashi <sup>\*†‡</sup>, Donghyun Son <sup>||</sup> and Kazuhiro Marumoto <sup>§||</sup>

<sup>†</sup>*Graduate School of Natural Science and Technology, and, <sup>‡</sup>Research Center for Sustainable Energy and Technology, Kanazawa University, Kakuma-machi, Kanazawa, Ishikawa 920-1192, Japan*

<sup>§</sup>*Japan Science and Technology Agency (JST), PRESTO, 4-1-8 Honcho Kawaguchi, Saitama 332-0012, Japan*

<sup>||</sup>*Institute of Materials Science, University of Tsukuba, Tsukuba, Ibaraki 305-8573, Japan*

\* Corresponding authors: Tel: +81-76-234-4770 (T. Kuwabara)

Fax: +81-76-234-4800 (T. Kuwabara)

E-mail: [tkuwabar@se.kanazawa-u.ac.jp](mailto:tkuwabar@se.kanazawa-u.ac.jp) (T. Kuwabara)

E-mail: [ktakaha@se.kanazawa-u.ac.jp](mailto:ktakaha@se.kanazawa-u.ac.jp) (K. Takahashi)

Submitted to *Journal of Physical Chemistry C*

## Abstract

In the glass-indium tin oxide (ITO) / titanium oxide ( $\text{TiO}_x$ ) / regioregular poly(3-hexylthiophene) (P3HT) : [6,6]-phenyl  $\text{C}_{60}$  butyric acid methyl ester (PCBM) / poly(3,4-ethylenedioxyethiophene) : poly(4-styrene sulfonic acid) (PEDOT:PSS) / Au cell ( $\text{TiO}_x$  cell), which contains amorphous titanium oxide prepared by chemical bath deposition and dried at 150 °C, a light soaking effect has been observed upon irradiation with white light. In contrast, in ITO / titanium oxide ( $\text{TiO}_2$ ) / P3HT:PCBM / PEDOT:PSS / Au cell ( $\text{TiO}_2$  cell), which contains anatase titanium oxide prepared by heat treatment at 450 °C, the maximum power conversion efficiency was obtained just after irradiation with white light. The number of  $\text{P3HT}^+$  cation radicals in the quartz-ITO/ $\text{TiO}_x$  and  $\text{TiO}_2$ /P3HT:PCBM substrates was estimated by ESR measurements at room temperature upon irradiation with white light. They increased gradually with an increase in irradiation time for the  $\text{TiO}_x$  substrate, but increased only slightly just after light irradiation for the  $\text{TiO}_2$  substrate. Upon irradiation with UV-cut light, the performance of the  $\text{TiO}_x$  cell was inferior to that of the  $\text{TiO}_2$  cell. This could be related to the resistances of the P3HT:PCBM layers which were estimated by alternating-current impedance spectroscopy. The resistance of the P3HT:PCBM layer in the  $\text{TiO}_x$  cell was much larger than that in the  $\text{TiO}_2$  cell, though the difference between the two cells was merely heat treatment temperature of titanium oxide films using as electron collection layers. That is, the concentration of photocarriers in the P3HT:PCBM of the  $\text{TiO}_x$

cell was significantly less than that in the P3HT:PCBM of the TiO<sub>2</sub> cell. From these experimental results, the light soaking effect could be reasonably explained by assuming the existence of charge recombination centers in the TiO<sub>x</sub> near the TiO<sub>x</sub>/P3HT:PCBM interface.

KEYWORDS: *Inverted solar cell, Titanium oxide, Polymer solar cell, Light soaking effect, Impedance spectroscopy, Electron spin resonance*

## **Introduction**

Because organic thin film solar cells are lightweight and flexible and can be manufactured cheaply, they have attracted much attention as next generation solar cells. Inverted organic solar cells that use chemically stable components in air as electrodes have attracted special attention<sup>1-5</sup>. These organic solar cells contain several very thin films that are laminated several times over; that is, two or more interfaces exist in the cell<sup>1,6-9</sup>. Therefore, the interface charge transport may become the main factor that influences cell performance. In inverted solar cells that contain sol-gel titanium oxide as an electron collection layer, a light soaking effect that cell performance improves gradually with an increase in light irradiation time has often been observed<sup>10-16</sup>. Although this mysterious phenomenon is now well known, there is not necessarily satisfactory explanation for the mechanism.

The light soaking effect has also been observed in inverted organic solar cells that contain amorphous titanium oxide, prepared by a chemical bath deposition process

(CBD-TiO<sub>x</sub>), as the electron collection layer<sup>17,18</sup>. Alternating-current impedance spectroscopic (IS) measurements can be used to quantify the electric properties of bulk and interface materials that cannot be determined using a direct current method. This is because the electric response speed for each component is different on the microscopic time scale. We previously investigated inverted solar cells containing metal oxides as electron collection electrodes by IS<sup>11,18-21</sup>. Electron spin resonance (ESR) is also a promising method for the microscopic characterization of charge-accumulation sites because it is a highly sensitive and powerful approach. The investigation of organic materials at the molecular level is thus possible. The ESR method has successfully been used to determine the microscopic properties of charge-carrier states in organic devices, including spin states and the spatial extent of wave functions in organic materials at device interfaces. We have previously investigated the accumulation of photo-generated charge carriers in conventional polymer solar cells under typical device operating conditions using the ESR method<sup>22-25</sup>.

In the work reported in this paper, we attempted to determine the mechanism of light soaking effect by investigating the features of the interface between the CBD-TiO<sub>x</sub> and the organic photoactive layer, using both ESR and IS.

## **2. Experimental Section**

### **2.1. Materials**

Titanium(IV) oxysulfate ( $\text{TiOSO}_4$ ), regioregular P3HT, PEDOT:PSS 1.3 wt% dispersion in water, Triton-X 100, and chlorobenzene (CB) were purchased from Sigma–Aldrich Chemical Co., Inc. Hydrogen peroxide ( $\text{H}_2\text{O}_2$ ) was purchased from Kanto Chemical Co., Inc. PCBM was purchased from Frontier Carbon Corporation. All chemicals were used as received. Glass-ITO substrates (sheet resistance =  $10 \Omega \text{ sq}^{-1}$ ) and Au wires were purchased from the Furuuchi Chemical Corporation. Glass-fluorine-doped tin oxide (FTO) substrates (A110U80, sheet resistance =  $12 \Omega \text{ sq}^{-1}$ ) were purchased from the AGC Fabritech Co., Ltd. Quartz substrates were purchased from Iiyama Precision Glass Co., Ltd. Indium-tin-oxide (ITO) layers (sheet resistance =  $\sim 10 \Omega \text{ sq}^{-1}$ ) on the quartz substrates were fabricated by Geomatec Co., Ltd.

## **2.2. Fabrication of inverted polymer solar cells**

The ITO and FTO electrodes were ultrasonicated in 2-propanol, and then cleaned in boiling 2-propanol, and subsequently dried in air. An amorphous titanium oxide film ( $\text{TiO}_x$ ) was prepared by the chemical bath deposition method described in our previous papers<sup>17,18</sup>. A  $\text{TiOSO}_4$  solution was added to a  $\text{H}_2\text{O}_2$  aqueous solution, and then the mixed solution was diluted to 50 ml with ultrapure water. The concentrations of  $\text{H}_2\text{O}_2$  and  $\text{TiOSO}_4$  were adjusted to 0.03 M, respectively. This solution was transferred to a screw vial to use as the reaction bath for film deposition. The glass side of the ITO and FTO substrates was covered with

imide tape to prevent the extra deposition of  $\text{TiO}_x$  precursor, and then the substrates were immersed in the bath at  $80\text{ }^\circ\text{C}$ . The solution became cloudy upon the application of heat, and after dipping for 10 min starting from this cloudy point, the immersed substrate was pulled out of the bath. The film thickness was about 30 nm. The as-deposited  $\text{TiO}_x$  precursor film on the electrodes was ultrasonicated for 10 min in water and heated at 150, 250, 350 and  $450\text{ }^\circ\text{C}$  for 1 h. The transparent conducting substrate used to prepare the solar cells was composed of the ITO heated at  $150\text{ }^\circ\text{C}$  and the FTO heated at 250, 350 and  $450\text{ }^\circ\text{C}$ . The precursor film was converted to  $\text{TiO}_x$  or anatase titanium(IV) oxide ( $\text{TiO}_2$ ) by heat treatment. A mixed CB solution containing P3HT and PCBM (weight ratio = 5:4) was spin-coated onto the  $\text{TiO}_x$  and  $\text{TiO}_2$  films. A PEDOT:PSS dispersion in water containing 0.5 wt.% Triton-X 100 was spin-coated onto the P3HT:PCBM layer. Film thicknesses were about 250 nm for the P3HT:PCBM layer and approximately 150 nm for PEDOT:PSS. An Au back electrode with a thickness of about 150 nm was vacuum deposited at  $2 \times 10^{-5}$  Torr onto the PEDOT:PSS layer. Finally, the cells were annealed at  $150\text{ }^\circ\text{C}$  for 5 min on a hot plate. The effective area of the solar cells was restricted to  $1\text{ cm}^2$  by depositing the Au electrode using a shadow mask.

### **2.3. Measurements**

The I-V curves of the solar cells were measured by linear sweep voltammetry at a scan rate of  $5\text{ V min}^{-1}$  under AM 1.5G- $100\text{ mW cm}^{-2}$  simulated sunlight irradiation or under

UV-cut light (light intensity:  $91.8 \text{ mW cm}^{-2}$ ) produced by excluding wavelengths less than 420 nm with a UV-cutoff filter. The light source was a SAN-EI Electric XES-502S solar simulator, which was calibrated using a standard silicon photovoltaic detector. All DC electric measurements were made using a Hokuto Denko HZ-5000 electrochemical analyzer. The IS measurements were obtained using an Agilent Technologies E4980A precision LCR meter in the dark and under simulated sunlight irradiation. The frequency range was from 20 Hz to 1 MHz, and the alternating signal magnitude was 5 mV. The data obtained were fitted with Scribner Associates Z-VIEW software v3.1 using the appropriate equivalent circuits. These measurements were carried out under an ambient atmosphere (ca.  $25 \text{ }^\circ\text{C}/40\text{--}60 \text{ \% RH}$ ).

X-ray diffraction (XRD) measurements were carried out using an X-ray diffractometer (Rigaku SmartLab) with Cu  $K\alpha$  radiation at  $45 \text{ kV} \times 200 \text{ mA}$ . Here, titanium oxide films for XRD measurement were prepared by repeating the chemical bath deposition onto FTO ten times. The film thickness was about 300 nm. ESR measurements were performed using a JEOL JES-FA200 X-band spectrometer under a nitrogen atmosphere at room temperature. ESR measurements under AM 1.5G light with  $100 \text{ mW cm}^{-2}$  intensity were obtained using a Bunkoukeiki OTENTOSUN-150BXM solar simulator. The number of spins and  $g$  values of the ESR signal were calibrated using a standard  $\text{Mn}^{2+}$  marker sample.

### **3. Results and Discussion**

### **3-1. Characteristics of the inverted polymer solar cells upon irradiation with white light.**

Figure 1 shows the time-dependence of the photo I-V curves under white light irradiation for inverted polymer solar cells containing the titanium oxide as an electron collection layer. In the  $\text{TiO}_x$  cells that contain titanium oxide prepared by heat treatment at 150 °C, the photovoltaic effect was hardly observed just after irradiation with white light. However, when light irradiation continued for the  $\text{TiO}_x$  cells, the photovoltaic effect gradually increased as shown in Figure 1a, which mainly improved the short-circuit photocurrent ( $J_{sc}$ ) and the fill factor (FF). The magnified I-V curves in the dark and just after irradiation for the  $\text{TiO}_x$  cell was shown in Figure 1c. Though the open-circuit voltage ( $V_{oc}$ ) obtained after irradiation for 15 sec was about 0.22 V, it reached the constant value of 0.57 V after irradiation for more than 1 min. When the  $\text{TiO}_x$  cell was remeasured under white light irradiation after stored in air and in the dark, such a light soaking effect was observed although the speed of improving the performance depended on the stored time of the cell. In contrast, in the case of the  $\text{TiO}_2$  cells with titanium oxide prepared by heat treatment at 450 °C, the maximum power conversion efficiency (PCE) was obtained just after white light irradiation, as shown in Figure 1b.

We confirmed crystal characteristics of titanium oxide, because the time-dependence of the photo I-V curves greatly depended on heating temperature of titanium oxide films as

mentioned above. The XRD patterns of the titanium oxide films on the FTO electrode after heating at more than 350 °C gave weak peak at  $2\theta = 25.2^\circ$  with an orientation along the (101) plane, as shown in Fig. 2. The  $\text{TiO}_2$  films were thus assigned to an anatase-type crystal structure. In contrast, the XRD patterns of the titanium oxide films after heating at less than 250 °C showed no peaks, indicating an amorphous phase.

ESR method was used to characterize the titanium oxide/P3HT:PCBM interface at room temperature for both quartz-ITO/ $\text{TiO}_x$ /P3HT:PCBM and quartz-ITO/ $\text{TiO}_2$ /P3HT:PCBM substrates. We can detect an ESR signal of  $\text{P3HT}^{+\cdot}$  cation radicals, though it is known that signals of radicals which are derived from titanium oxide and PCBM are not detected under room temperature<sup>22,25</sup>. Figure 3a shows ESR spectra obtained under dark conditions, under UV-cut light irradiation, and under white light irradiation for the quartz-ITO/ $\text{TiO}_x$ /P3HT:PCBM substrate. Under dark conditions, a clear but small ESR signal was observed for the substrate. The ESR parameters obtained were the  $g$  value and the peak-to-peak linewidth ( $\Delta H_{pp}$ ) and they were  $g = 2.002$  and  $\Delta H_{pp} = 0.253$  mT, respectively. The  $\text{P3HT}^{+\cdot}$  cation radicals were thus produced upon the oxidation of  $\text{P3HT}^{22}$ . Such a similar result was also obtained for the quartz-ITO/ $\text{TiO}_2$ /P3HT:PCBM substrate under dark conditions. This likely comes from the partial formation of a  $\text{P3HT}^+:\text{PCBM}^-$  charge-transfer complex in the ground state and the physical adsorption of oxygen onto P3HT:PCBM, which then functions as an electron acceptor. Figure 3b shows the time-dependence of the number of

radical spins ( $N_{\text{spin}}$ ) that originates from  $\text{P3HT}^{+\cdot}$  under light irradiation. When irradiated with UV-cut light which excluded ultraviolet rays of less than 420 nm, the ESR signal intensity of both the quartz-ITO/ $\text{TiO}_x$ /P3HT:PCBM and quartz-ITO/ $\text{TiO}_2$ /P3HT:PCBM substrates increased slightly by a photo-charge separation, as shown in zones I and II of Figure 3b. When irradiated with UV-containing white light subsequently in zone III, the number of radicals increased with an increase in irradiation time for the quartz-ITO/ $\text{TiO}_x$ /P3HT:PCBM substrate. In contrast, it did not increase anymore in zone III for the quartz-ITO/ $\text{TiO}_2$ /P3HT:PCBM substrate. This difference between the two substrates suggests the presence of electron trap sites in the  $\text{TiO}_x$ . Upon the band gap excitation of the  $\text{TiO}_x$  by UV light being contained in white light, electrons are excited from the valence band to the conduction band because the  $\text{TiO}_x$  film has light absorption at wavelength of less than 380 nm. Subsequently the electrons are partially captured in above mentioned trap sites and consequently long-life holes accumulate in the valence band. The holes in the  $\text{TiO}_x$  near the  $\text{TiO}_x$ /P3HT:PCBM interface can oxidize the P3HT slowly across the interface. As another possibility, adsorbed oxygen molecules on the  $\text{TiO}_x$  by an interaction with the trap sites are desorbed by UV light exposure, and the released oxygen molecules can dope the P3HT. In either case, the number of radicals that originates from  $\text{P3HT}^{+\cdot}$  increase gradually with an increase in irradiation time. However, because there is little number of the electron trap sites in the  $\text{TiO}_2$ , the excited electrons in the conduction band rapidly recombine

with the holes that formed in the valence band, that is, long-life holes hardly produce in the valence band. In addition, oxygen molecules are hardly adsorbed on the  $\text{TiO}_2$ . Thus, in the quartz-ITO/ $\text{TiO}_2$ /P3HT:PCBM substrate, the number of  $\text{P3HT}^{+\cdot}$  radicals does not increase by irradiation with white light in zone III. In last Zone I under dark conditions, the number of radicals in the quartz-ITO/ $\text{TiO}_x$ /P3HT:PCBM substrate decreased rapidly first and decreased slowly afterwards. This is perhaps because the recombination rate between  $\text{P3HT}^{+\cdot}$  radicals and trapped electrons in  $\text{TiO}_x$  is slow when the trapped position is away from the  $\text{TiO}_x$ /P3HT:PCBM interface.

The light soaking effect on the  $\text{TiO}_x$  cell under white light irradiation was observed as an increase in photocurrent and FF, as shown in Figure 1a. To further characterize this effect, IS measurements were carried out by applying a DC bias of 0.5 V to the cell. Figure 4 shows typical Nyquist plots of the  $\text{TiO}_x$  cell under white light irradiation. The plots consist of an arc at a high frequency of more than 30 kHz and a second arc at a low frequency of less than 30 kHz. The former and the latter are denoted arc 1 and arc 2, respectively. The plots were analyzed using the equivalent circuit shown in the inset of Figure 4, and a reasonable fit to the simulated curve was obtained.  $R_s$  represents the series resistance that consists of ohmic components.  $R_1$  and  $R_2$  are resistance components that form a parallel circuit with the constant phase elements (CPE1 and CPE2). According to our previous papers<sup>11,18,19</sup>, arcs 1 and 2 can be assigned to components related to titanium oxide and P3HT:PCBM, respectively.

The arc size decreases with an increase in irradiation time. To further clarify the relationship between the resistance components and the photocurrent, Figures 1a and 4 were rearranged as shown in Figure 5. The photocurrent continuously increases with an increase in the irradiation time and this corresponds to a decrease in both R1 and R2. Kim et al.<sup>26</sup> reported that the emergence of photoconduction of titanium oxide films mirrored the increase and gradual saturation of the photocurrent of TiO<sub>x</sub> cells. This may be supported by the decrease in R1. On the contrary, Trost et al.<sup>15</sup> insisted that the origin of the light-soaking effect was the TiO<sub>x</sub>/organic interface which had an energy barrier for the electron extraction. Further it was reported in recent work<sup>16,27-29</sup> that the light-soaking effect was observed because the energy barrier at such an interface reduced with an increase in light irradiation time. In addition, we think that the existence of electron trap sites in TiO<sub>x</sub> near the TiO<sub>x</sub>/P3HT:PCBM interface, which was suggested by ESR measurements, can become one of the reasons for the light-soaking effect.

### **3-2. Characteristics of the inverted polymer solar cells upon irradiation with UV-cut light.**

To exclude the influence of photoconduction of titanium oxide films on the photovoltaic effect, we examined the characteristics of TiO<sub>x</sub> and TiO<sub>2</sub> cells upon irradiation with UV-cut light, which excluded ultraviolet rays of less than 420 nm. Figure 6 shows I-V

curves after light irradiation of 30 min for the inverted polymer solar cells that contain titanium oxide prepared at various heat treatment temperatures upon irradiation with white light (a) and UV-cut light (b). When irradiated with white light, the I-V curves showed a good *J* shape and the PCE was about 3.4% irrespective of treatment temperature. This shows that the titanium oxides effectively act as electron collection layers. However, when irradiated by UV-cut light, the performance remarkably depends on the treatment temperature. For the TiO<sub>x</sub> prepared by heating at 150 and 250 °C, an I-V curve with a *S* shape, that is, high series resistance was observed, resulting in a low PCE. In particular, a remarkably small V<sub>oc</sub> of about 0.25 V was obtained only for the cell containing the TiO<sub>x</sub> prepared by heating at 150 °C as shown in Figure 6b, though the V<sub>oc</sub> of the cells containing the titanium oxides prepared by heating at 250, 350 and 450 °C was almost the same value of about 0.57 V. This suggests that the electron trap sites in the TiO<sub>x</sub> near the TiO<sub>x</sub>/P3HT:PCBM interface function as recombination centers for the photo-produced charge carriers in P3HT:PCBM. Conversely, for the TiO<sub>2</sub> prepared by heating at 350 and 450 °C, an I-V curve with a *J* shape was observed and it gave relatively large PCEs. Perhaps because many hydroxyl groups in TiO<sub>x</sub>, which act as the recombination centers, reduce by a dehydration reaction upon heat treatment at more than 350 °C, the charge recombination centers becomes very few in the TiO<sub>2</sub>. This is supported by the ESR measurements, which suggest that the number of electron trap sites in the TiO<sub>2</sub> is significantly less than those in the TiO<sub>x</sub>.

The arc size of Nyquist plots for the  $\text{TiO}_x$  cell under short-circuit conditions gradually decreased with an increase in irradiation time, then it became almost constant after light soaking for more than 30 min. Figure 7 shows the saturated plots that were obtained under short-circuit conditions for the inverted polymer solar cells containing the titanium oxides prepared at various treatment temperatures. These plots were analyzed using the equivalent circuit shown in the inset of Figure 4, and a reasonable fit to the simulated curve was obtained. The plots consist of arc 1 at a high frequency of more than 60 kHz and arc 2 at a low frequency of less than 60 kHz. Upon irradiation with white light, the arc sizes were similar irrespective of treatment temperature, as shown in Figure 7a. This result is consistent with the I-V behavior shown in Figure 6a. Conversely, upon irradiation with UV-cut light, the size of arc 2 decreased with an increase in treatment temperature, as shown in Figure 7b. This corresponds to the I-V behavior shown in Figure 6b.

To explain the changes in the Nyquist plots under UV-cut light, the relationship between the resistance components ( $R_1$ ,  $R_2$ ) and the short-circuit photocurrent ( $J_{sc}$ ) is summarized in Figure 8 using the data from Figures 6b and 7b. Here  $R_1$  and  $R_2$  originate from the resistances of titanium oxide film which absorbs no visible light and the P3HT:PCBM layer which absorbs it, respectively<sup>11,18,19</sup>. Nyquist plot that was obtained in the dark for the cell containing the  $\text{TiO}_x$  prepared at treatment temperature of 150 °C was shown in the inset of Figure 7a, reasonably fitting to the simulated curve using the equivalent circuit

shown in the inset of Figure 4. The R2 remarkably decreased from  $81 \text{ k}\Omega \text{ cm}^2$  in the dark to  $30 \text{ }\Omega \text{ cm}^2$  under white light irradiation and to  $450 \text{ }\Omega \text{ cm}^2$  under UV-cut light. This supports that the R2 originates from P3HT:PCBM layer which has large photoconductivity because of a photo-induced intermolecular charge transfer. Because R1 was much smaller than R2, the change in  $J_{sc}$  was discussed by considering R2 which had slow frequency response. The R2 decreased with the increase in the titanium oxide treatment temperature, that is, the concentration of photo-carriers in P3HT:PCBM increased with the increase in the treatment temperature. This could be reasonably explained by assuming the existence of charge recombination centers in the  $\text{TiO}_x$  near the  $\text{TiO}_x$ /P3HT:PCBM interface. On the other hand, because the electrons produced by the bandgap excitation of  $\text{TiO}_x$  upon irradiation with UV light are closer to the recombination centers than those produced by the photo-excitation of P3HT:PCBM, these centers were filled preferentially and gradually by the electrons produced by the bandgap excitation of  $\text{TiO}_x$ . Therefore, in addition to the photoconductivity of  $\text{TiO}_x$ , the light soaking effect is observed because of the slow disappearance of the recombination centers, mainly accompanying the increase in the photocurrent and the fill factor. Lin et al.<sup>13</sup> observed that when  $\text{TiO}_x$  cells after light soaking were stored in air for 3 h under the dark, the photo I-V curve returned from *J* shape to *S* shape. However such a change was hardly observed when stored in high vacuum of  $8 \times 10^{-7}$  Torr for 18 h. They inferred that there were surface  $\text{Ti}^{3+}$  states returning to  $\text{Ti}^{4+}$  states on  $\text{O}_2$  adsorption, which caused the conductivity of

the  $\text{TiO}_x$  film to decrease and the  $S$  shape to return back. Such surface  $\text{Ti}^{4+}$  states may be equivalent to the recombination centers which we mentioned above, although the ESR signal which came from such defects was not observed at room temperature<sup>25</sup>.

#### 4. Conclusion

We found that the number of  $\text{P3HT}^+$  cation radicals in a quartz-ITO/ $\text{TiO}_x$ /P3HT:PCBM substrate, which was estimated by ESR at room temperature, increased gradually with an increase in irradiation time upon irradiation with UV-containing white light. This result can be reasonably explained by assuming the existence of electron trap sites in the  $\text{TiO}_x$ . The PCE of the  $\text{TiO}_x$  and  $\text{TiO}_2$  cells upon irradiation with UV-cut light correlated well with the resistance of the P3HT:PCBM layers, which was estimated by IS measurements in a low frequency range. The resistance of the organic active layer in the  $\text{TiO}_x$  cell was much larger than that in the  $\text{TiO}_2$  cell, that is, the concentration of photo-carriers in the mentioned P3HT:PCBM was significantly smaller than that in the latter. We infer from these discussion that the electron trap sites existing in the  $\text{TiO}_x$  near the  $\text{TiO}_x$ /PCBM:P3HT interface act as recombination centers for photo-produced electrons and holes from the P3HT:PCBM layer. However, because the electrons that are produced by the bandgap excitation of the  $\text{TiO}_x$  upon irradiation with UV light can fill the recombination centers, the light soaking effect improving the photovoltaic properties is observed.

## ACKNOWLEDGMENT

This work was supported by the Japan Society for the Promotion of Science (JSPS) KAKENHI Grants-in-Aid for Scientific Research (B) and for Young Scientists (A), (Grant No. 24350092 and 25708029, respectively), Japan.

## REFERENCES

- (1) Chen, L.-M.; Hong, Z.; Li, G.; Yang, Y. Recent Progress in Polymer Solar Cells: Manipulation of Polymer:Fullerene Morphology and the Formation of Efficient Inverted Polymer Solar Cells. *Adv. Mater.* **2009**, *21*, 1434-1449.
- (2) Jørgensen, M.; Norrman, K.; Krebs, F. C. Stability/Degradation of Polymer Solar Cells. *Sol. Energy Mater. Sol. Cells* **2008**, *92*, 686-714.
- (3) He, Z.; Zhong, C.; Su, S.; Xu, M.; Wu, H.; Cao, Y. Enhanced Power-Conversion Efficiency in Polymer Solar Cells Using an Inverted Device Structure. *Nat. Photon.* **2012**, *6*, 591-595.
- (4) Jørgensen, M.; Norrman, K.; Gevorgyan, S. A.; Tromholt, T.; Andreasen, B.; Krebs, F. C. Stability of Polymer Solar Cells. *Adv. Mater.* **2012**, *24*, 580-612.
- (5) Lee, J. U.; Jung, J. W.; Jo, J. W.; Jo, W. H. Degradation and Stability of Polymer-Based Solar Cells. *J. Mater. Chem.* **2012**, *22*, 24265-24283.
- (6) Günes, S.; Neugebauer, H.; Sariciftci, N. S. Conjugated Polymer-Based Organic Solar Cells. *Chem. Rev.* **2007**, *107*, 1324-1338.
- (7) Thompson, B. C.; Fréchet, J. M. J. Polymer–Fullerene Composite Solar Cells. *Angew. Chem. Int. Ed.* **2008**, *47*, 58-77.
- (8) Park, S. H.; Roy, A.; Beaupre, S.; Cho, S.; Coates, N.; Moon, J. S.; Moses, D.; Leclerc, M.; Lee, K.; Heeger, A. J. Bulk Heterojunction Solar Cells with Internal Quantum Efficiency Approaching 100%. *Nat. Photon.* **2009**, *3*, 297-302.
- (9) Ma, H.; Yip, H.-L.; Huang, F.; Jen, A. K. Y. Interface Engineering for Organic Electronics. *Adv. Funct. Mater.* **2010**, *20*, 1371-1388.
- (10) Kuwabara, T.; Nakayama, T.; Uozumi, K.; Yamaguchi, T.; Takahashi, K. Highly Durable Inverted-Type Organic Solar Cell Using Amorphous Titanium Oxide as Electron Collection Electrode Inserted between ITO and Organic Layer. *Sol. Energy Mater. Sol. Cells* **2008**, *92*, 1476-1482.
- (11) Kuwabara, T.; Iwata, C.; Yamaguchi, T.; Takahashi, K. Mechanistic Insights into UV-Induced Electron

Transfer from PCBM to Titanium Oxide in Inverted-Type Organic Thin Film Solar Cells Using AC Impedance Spectroscopy. *ACS Appl. Mater. Interfaces* **2010**, *2*, 2254-2260.

(12) Kim, J.; Kim, G.; Choi, Y.; Lee, J.; Heum Park, S.; Lee, K. Light-Soaking Issue in Polymer Solar Cells: Photoinduced Energy Level Alignment at the Sol-Gel Processed Metal Oxide and Indium Tin Oxide Interface. *J. Appl. Phys.* **2012**, *111*, 114511.

(13) Lin, Z.; Jiang, C.; Zhu, C.; Zhang, J. Development of Inverted Organic Solar Cells with TiO<sub>2</sub> Interface Layer by Using Low-Temperature Atomic Layer Deposition. *ACS Appl. Mater. Interfaces* **2013**, *5*, 713-718.

(14) Wong, K. H.; Mason, C. W.; Devaraj, S.; Ouyang, J.; Balaya, P. Low Temperature Aqueous Electrodeposited TiO<sub>x</sub> Thin Films as Electron Extraction Layer for Efficient Inverted Organic Solar Cells. *ACS Appl. Mater. Interfaces* **2014**, *6*, 2679-2685.

(15) Trost, S.; Zilberberg, K.; Behrendt, A.; Polywka, A.; Görm, P.; Reckers, P.; Maibach, J.; Mayer, T.; Riedl, T. Overcoming the "Light-Soaking" Issue in Inverted Organic Solar Cells by the Use of Al:ZnO Electron Extraction Layers. *Adv. Energy Mater.* **2013**, *3*, 1437-1444.

(16) Guerrero, A.; Chambon, S.; Hirsch, L.; Garcia-Belmonte, G. Light-Modulated TiO<sub>x</sub> Interlayer Dipole and Contact Activation in Organic Solar Cell Cathodes. *Adv. Funct. Mater.* **2014**, *24*, 6234-6240.

(17) Kuwabara, T.; Sugiyama, H.; Kuzuba, M.; Yamaguchi, T.; Takahashi, K. Inverted Bulk-Heterojunction Organic Solar Cell Using Chemical Bath Deposited Titanium Oxide as Electron Collection Layer. *Org. Electron.* **2010**, *11*, 1136-1140.

(18) Kuwabara, T.; Kuzuba, M.; Emoto, N.; Yamaguchi, T.; Taima, T.; Takahashi, K. Effect of the Solvent Used to Prepare the Photoactive Layer on the Performance of Inverted Bulk Heterojunction Polymer Solar Cells. *Jpn. J. Appl. Phys.* **2014**, *53*, 02BE06 01-04.

(19) Kuwabara, T.; Kawahara, Y.; Yamaguchi, T.; Takahashi, K. Characterization of Inverted-Type Organic Solar Cells with a ZnO Layer as the Electron Collection Electrode by ac Impedance Spectroscopy. *ACS Appl. Mater. Interfaces* **2009**, *1*, 2107-2110.

(20) Kuwabara, T.; Nakamoto, M.; Kawahara, Y.; Yamaguchi, T.; Takahashi, K. Characterization of ZnS-Layer-Inserted Bulk-Heterojunction Organic Solar Cells by ac Impedance Spectroscopy. *J. Appl. Phys.* **2009**, *105*, 124513.

(21) Kuwabara, T.; Tamai, C.; Omura, Y.; Yamaguchi, T.; Taima, T.; Takahashi, K. Effect of UV Light Irradiation on Photovoltaic Characteristics of Inverted Polymer Solar Cells Containing Sol-Gel Zinc Oxide Electron Collection Layer. *Org. Electron.* **2013**, *14*, 649-656.

(22) Nagamori, T.; Marumoto, K. Direct Observation of Hole Accumulation in Polymer Solar Cells During Device Operation using Light-Induced Electron Spin Resonance. *Adv. Mater.* **2013**, *25*, 2362-2367.

(23) Nagamori, T.; Marumoto, K. Charge Accumulation in Organic Solar Cells during Device Operation as Investigated by Electron Spin Resonance. *Jpn. J. Appl. Phys.* **2013**, *52*, 05DC13.

(24) Seki, K.; Marumoto, K.; Tachiya, M. Bulk Recombination in Organic Bulk Heterojunction Solar Cells under Continuous and Pulsed Light Irradiation. *Appl. Phys. Express* **2013**, *6*, 051603.

(25) Chiesa, M.; Paganini, M. C.; Livraghi, S.; Giamello, E. Charge Trapping in TiO<sub>2</sub> Polymorphs as Seen by Electron Paramagnetic Resonance Spectroscopy. *Phys. Chem. Chem. Phys.* **2013**, *15*, 9435-9447.

- (26) Kim, C. S.; Lee, S. S.; Gomez, E. D.; Kim, J. B.; Loo, Y.-L. Transient Photovoltaic Behavior of Air-Stable, Inverted Organic Solar Cells with Solution-Processed Electron Transport Layer. *Appl. Phys. Lett.* **2009**, *94*, 113302.
- (27) Tress, W.; Leo, K.; Riede, M. Influence of Hole-Transport Layers and Donor Materials on Open-Circuit Voltage and Shape of I–V Curves of Organic Solar Cells. *Adv. Funct. Mater.* **2011**, *21*, 2140-2149.
- (28) Tress, W.; Corvers, S.; Leo, K.; Riede, M. Investigation of Driving Forces for Charge Extraction in Organic Solar Cells: Transient Photocurrent Measurements on Solar Cells Showing S-Shaped Current–Voltage Characteristics. *Adv. Energy Mater.* **2013**, *3*, 873-880.
- (29) Tress, W.; Inganäs, O. Simple Experimental Test to Distinguish Extraction and Injection Barriers at the Electrodes of Organic Solar Cells with S-Shaped Current–Voltage Characteristics. *Sol. Energy Mater. Sol. Cells* **2013**, *117*, 599-603.

## Figures

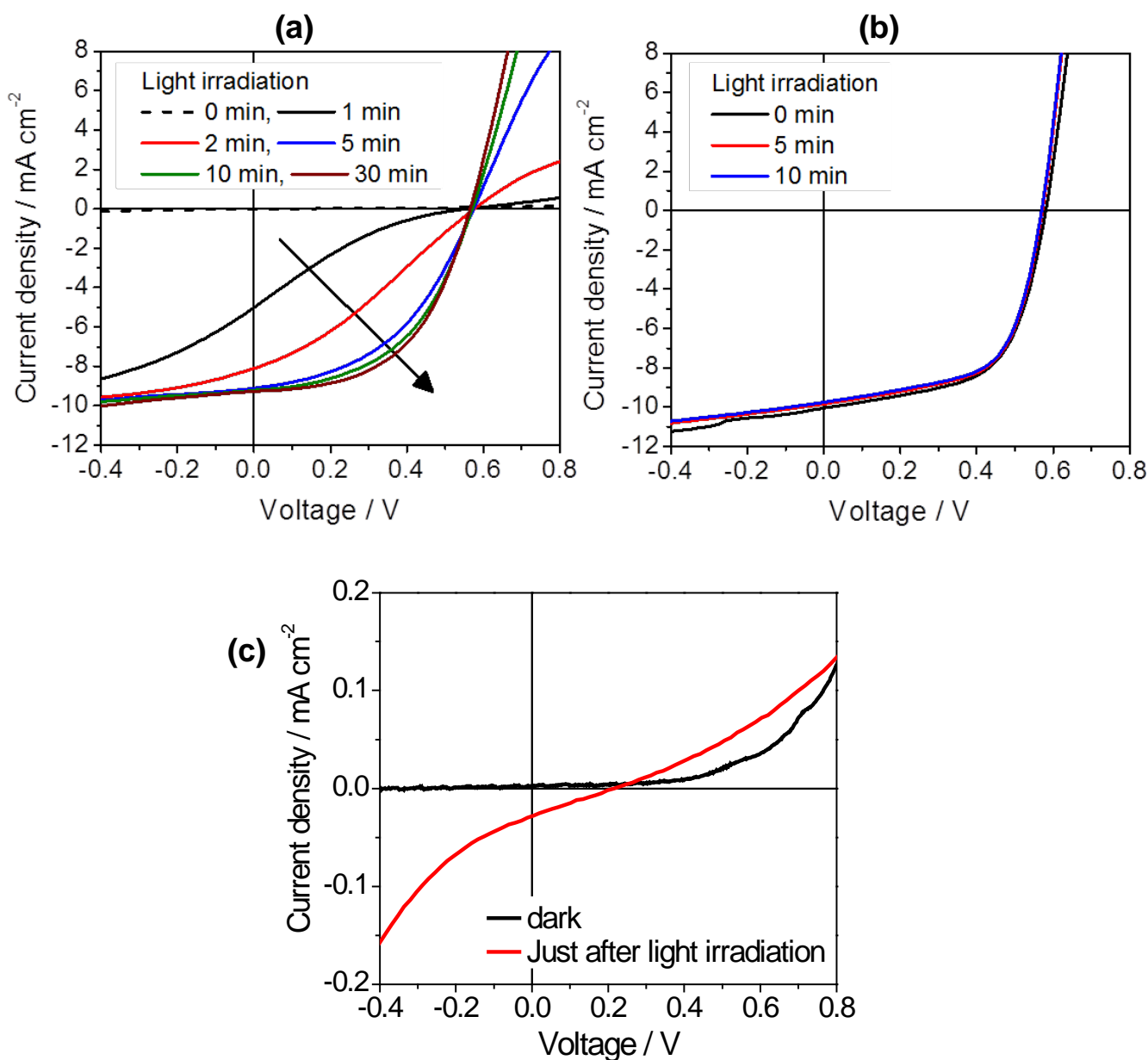


Figure 1 Time-dependence of the photo I-V curves under white light irradiation for the inverted polymer solar cells containing titanium oxide prepared by heat treatment at 150 °C (a) and 450 °C (b), and the magnified I-V curves in the dark and just after irradiation for TiO<sub>x</sub> cell (c). The explanatory notes showed the time when we started the I-V measurements after beginning white light irradiation. The start point of I-V curves was the applied voltage of -1 V.

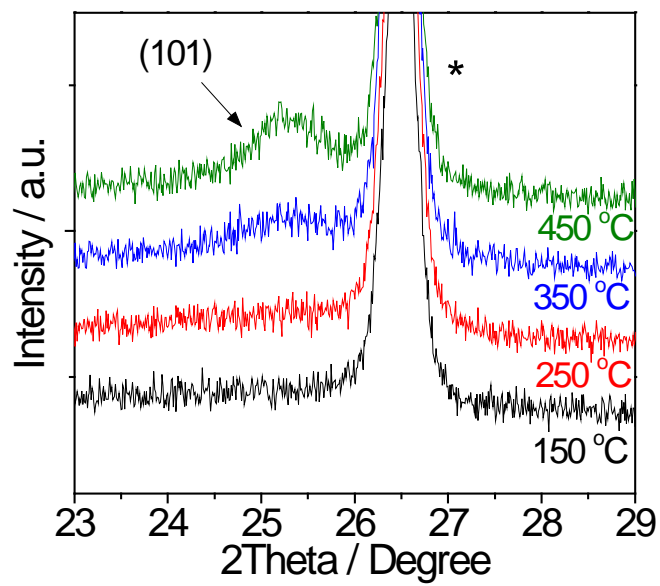


Figure 2 XRD spectra of the titanium oxide films on FTO substrates prepared at various heat treatment temperatures. Asterisk is diffraction peak of FTO.

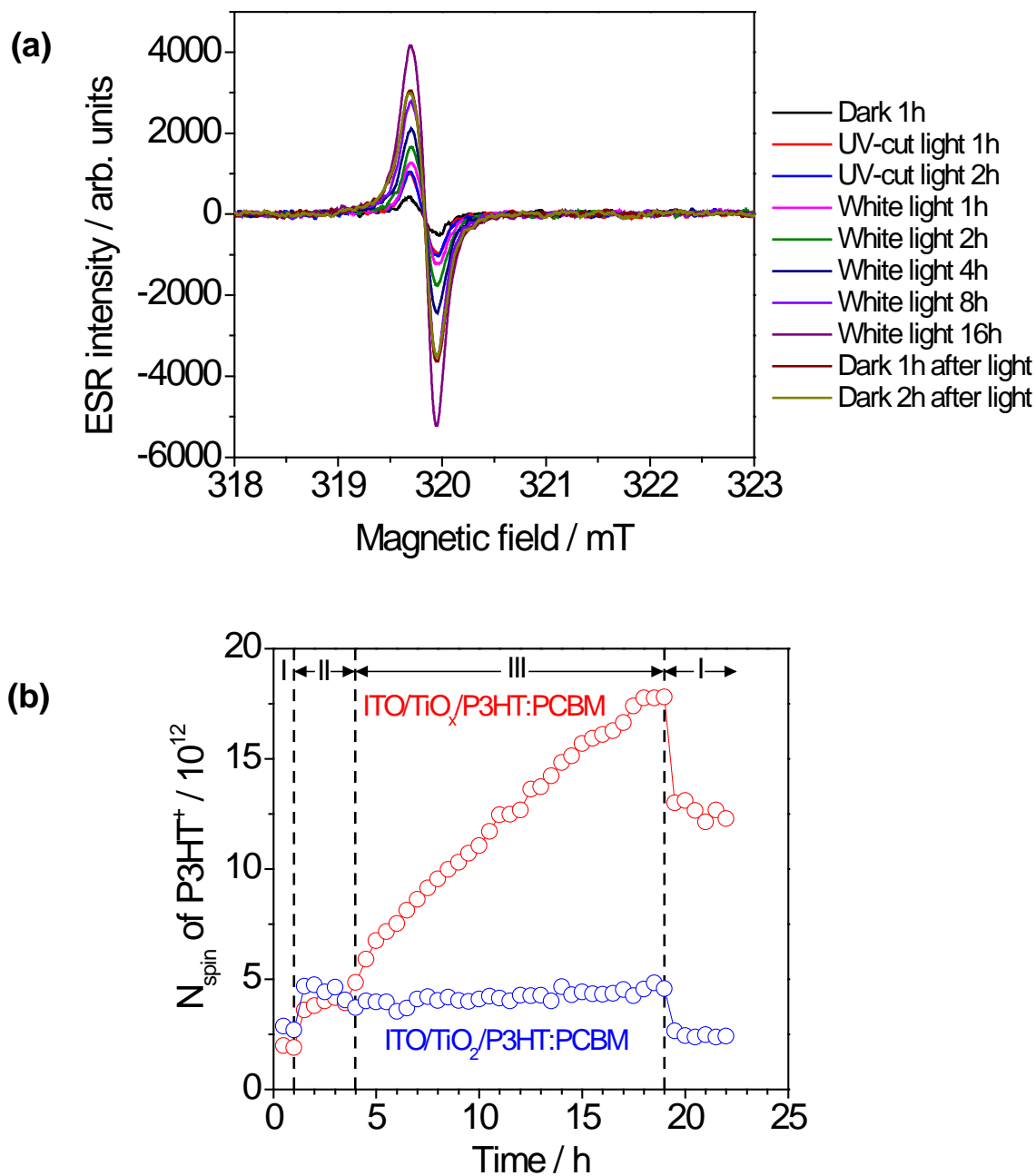


Figure 3 (a) ESR spectra obtained under dark conditions, under UV-cut light irradiation, and under white light irradiation for the quartz-ITO/TiO<sub>x</sub>/P3HT:PCBM substrate at room temperature. (b) Dependence of the radical spin number ( $N_{\text{spin}}$ ) of  $\text{P3HT}^{\cdot+}$  in the quartz-ITO/TiO<sub>x</sub> (○) substrate and the TiO<sub>2</sub> (○)/P3HT:PCBM substrates on light irradiation time. Zones I, II, and III are in the dark, under UV-cut light irradiation, and under white light irradiation, respectively.

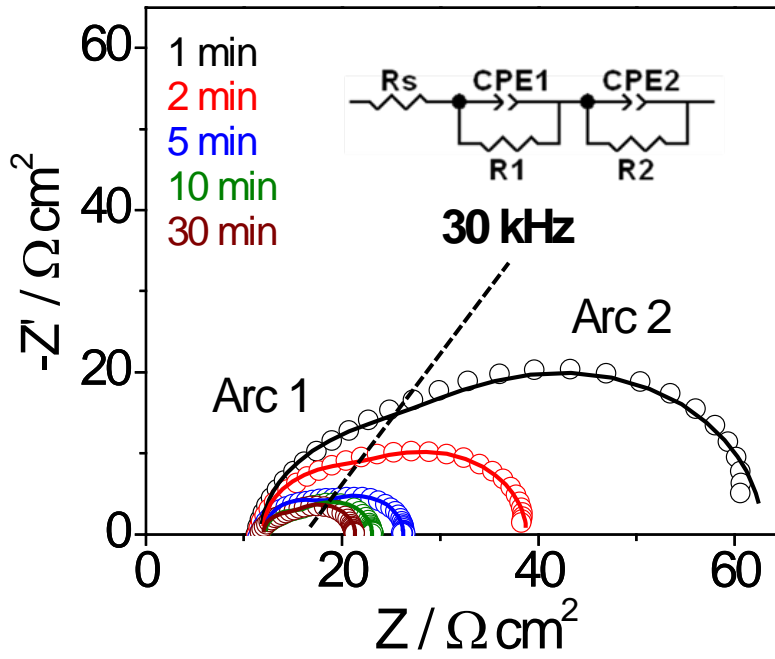


Figure 4 Typical Nyquist plots of the  $\text{TiO}_x$  cell at an applied voltage of 0.5 V after 1, 2, 5, 10 and 30 min of white light irradiation. Solid lines indicate the curves calculated using the equivalent circuit shown by the inset.

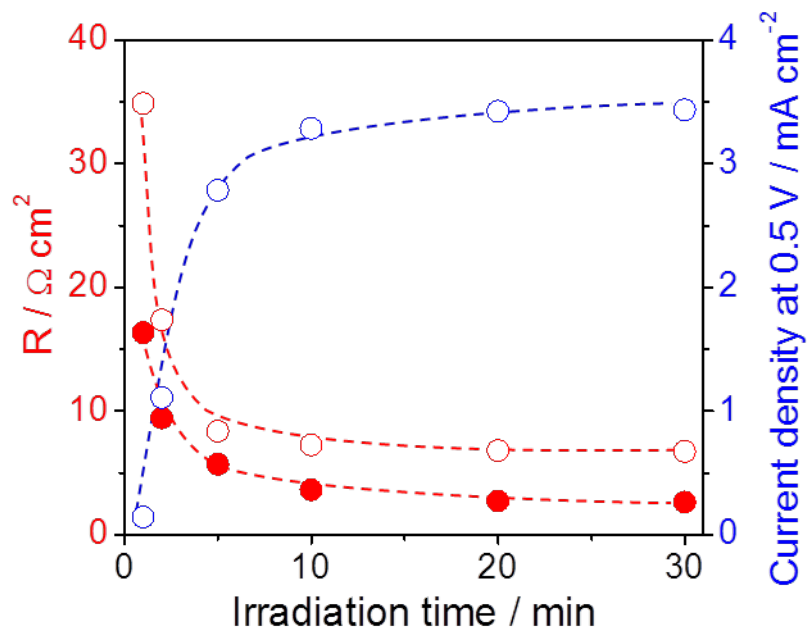


Figure 5 Time-dependence of R1 (●), R2 (○), and photocurrent (○) at an applied voltage of 0.5 V under white light irradiation for the  $\text{TiO}_x$  cell.

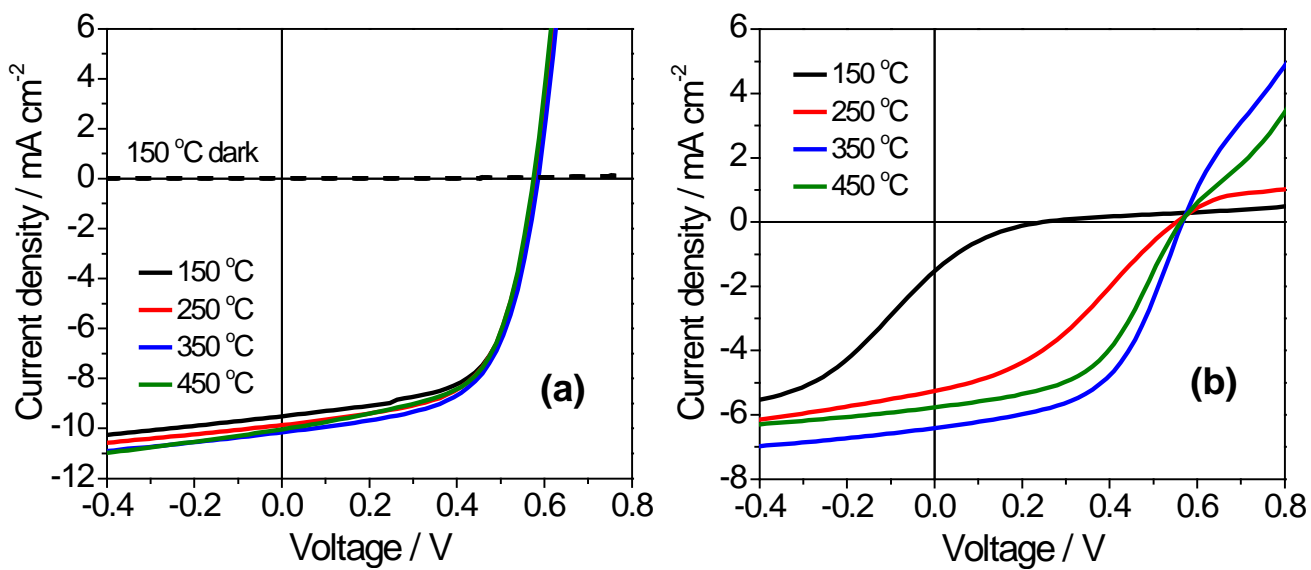


Figure 6 Photo I-V curves after light irradiation of 30 min for the inverted polymer solar cells containing titanium oxide prepared using various heat treatment temperatures under white light irradiation (a) and under UV-cut light irradiation (b).

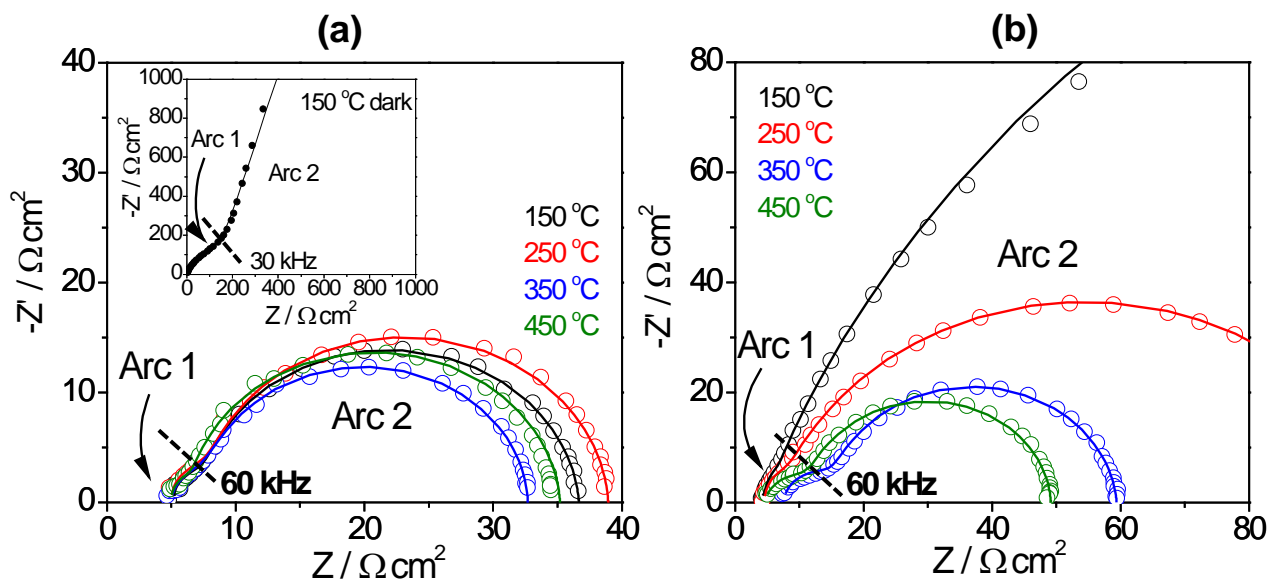


Figure 7 Nyquist plots obtained under the short-circuit conditions for the inverted polymer solar cells containing titanium oxide prepared at various heat treatment temperatures under white light irradiation (a) and under UV-cut light irradiation (b). These plots were almost constant during light irradiation from 30 min to 2 h. The inset of Figure 7a is Nyquist plot in the dark for the  $\text{TiO}_x$  cell containing titanium oxide prepared at heat treatment temperature of 150 °C. The solid lines indicate calculated curves obtained from the equivalent circuit shown in the inset of Figure 4.

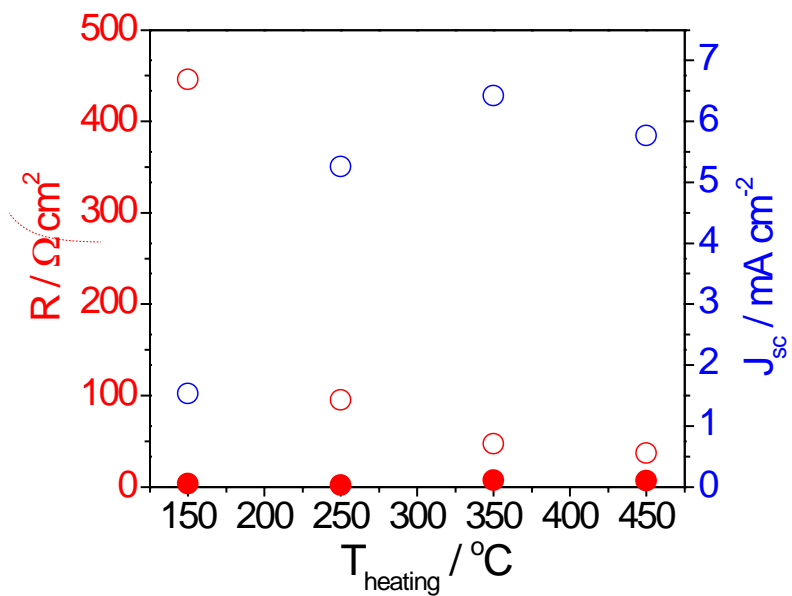


Figure 8 Plots of R1 (●), R2 (○) and photocurrent density (J<sub>sc</sub>:○) under short-circuit conditions for the inverted polymer solar cells containing titanium oxide prepared at various heat treatment temperatures. Cell irradiation was done using UV-cut light.

## TOC graphic

